

Aerodynamic performance improvement using a linear multi-spark pulsating plasma array

*Nina F. Yurchenko¹⁾ and Pavlo M. Vynogradsky²⁾

^{1), 2)} *Laboratory for Advanced Aerodynamics and Interdisciplinary Research, Institute of Hydromechanics, National Academy of Sciences of Ukraine, Kiev 03680, Ukraine*

¹⁾ nina.yurchenko@gmail.com

ABSTRACT

The concept of energy-efficient flow control is developed which is based on initiation and maintenance of an inherent to flow vortical structure with a given scale. It can be realized by means of different mechanisms and devices starting from spanwise arrays of roughness elements (passive flow control) to thermally induced regular temperature variation along a span (active flow control).

Linear arrays of multi-spark plasma flush mounted in the model created downstream thermal wakes ("thermal riblets"). Resultant flow restructuring was studied numerically while measured aerodynamic forces showed correlation between the modified flow structure and integral flow characteristics (lift, drag, pitch moment coefficients and pressure distributions). It served as a criterion of flow optimization around test models which could be both blunt bodies and a supercritical airfoil model.

Application of pulsating spark discharges showed that an optimal choice of plasma and flow parameters can result in growing values of lift coefficient and stall angle combined with drag reduction.

1. INTRODUCTION

The developed flow-control strategy [2, 4, 5, 6, 8] was realized using spanwise arrays of multi-spark plasma actuators [9]. Various earlier tested realizations of this strategy showed encouraging results in terms of aerodynamic performance improvement [5-9]. Designed flow-control devices generated a necessary controllable $U(z)$ disturbance field either mechanically or thermally. A key element of these devices is a z-oriented array of roughness elements [1], micro-jets [9], resistively [3] or microwave [5, 7] heated flush-

¹⁾ Ph.D., Laboratory Director

²⁾ Ph.D., Senior Researcher

mounted strips, microwave-generated [3, 5, 7] or high-voltage initiated [9] plasma discharges. Figs. 1 and 2 illustrate a streaky thermal pattern in a near-wall flow which can be considered as thermal “riblets”, directly heated flush-mounted streamwise strips or a similar array of thermal wakes downstream of plasma discharges.

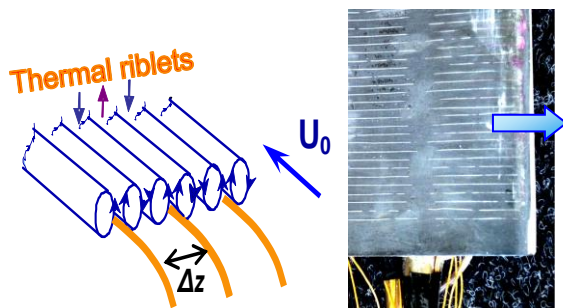


Fig. 1. Initiation of streamwise vortices with a given Δz space scale by means of selective surface heating, “thermal riblets” (left), and a model surface with embedded strips heated with applied voltage (right).

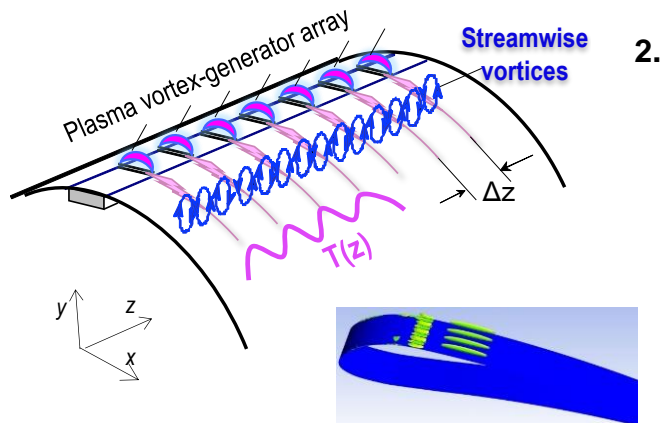


Fig. 2. Sketch and numerical pattern of “virtual thermal riblets” consisting of an array of Δz -spaced heated wakes downstream of high-temperature plasma discharges

RESULTS AND DISCUSSION

Investigations are planned and implemented as combined numerical and experimental studies. Numerical simulation aims at determination and understanding of a flow structure affected by z -regular disturbers. It gives a guidance to choose optimal control parameters to minimize laborious experimental efforts. E.g. for microwave generated plasma discharges it was found a marginal spacing of $\Delta z = 1.33$ cm to provide an adequate, same space scale, flow response to vortex generation. Besides, optimal locations of the array were evaluated in the downstream direction (vicinity of the separation) and normally to the wall (outer edge of a boundary layer).

The downstream merge of the successively “radiated” streamwise vortices (see Fig. 2) in a pulse mode explained best measured aerodynamic coefficients obtained for the pulse repetition rate, $f=1000$ Hz, pulse duration $\tau=0.1$ ms, at $U_0=20$ m/s for near-critical angles of attack. Numerical and experimental studies demonstrated that similar to the localized surface heating, plasma arrays cause the development of streamwise vortices with a given scale as well as an improvement of the aerodynamic performance. Fig. 3

shows growing stall angles accompanied with the drag reduction within a certain range of angles of attack. The same effects were found for a circular cylinder in a crossflow tested at $U_0=15-40$ m/s and a few combinations of microwave radiation parameters, pulse duration, and pulse repetition rate.

Gradually accumulated experience and knowledge helped to effectively plan further investigations. Comparison of all tested flow-control devices designed in the framework of the mentioned concept and obtained results showed advantages of the multi-spark plasma

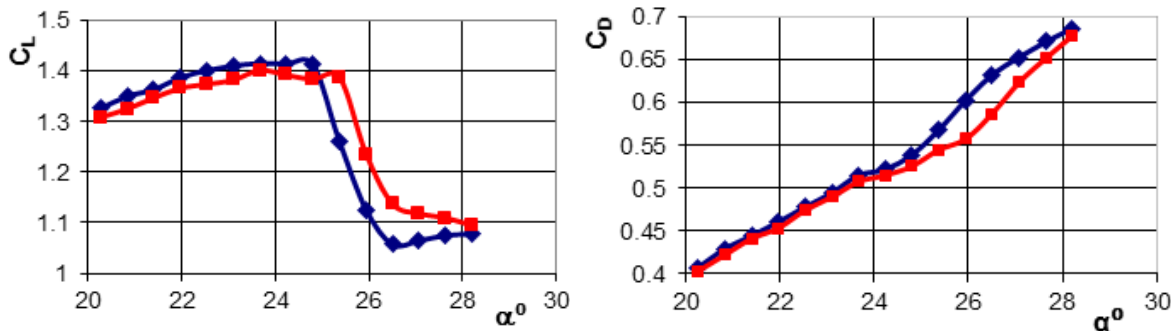


Fig. 3. Lift C_L and drag C_D coefficients depending on an angle of attack α of an airfoil model: red curves – measurements with z-regular plasma discharges, blue – reference case

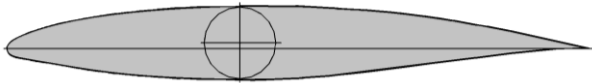


Fig. 4. Airfoil (SAP) model contours (top) and mounted spark plasma insert (bottom): 1 - left endplate; 2 - discharge gaps; 3 – pressure taps; 4 – plasma array insert.

array. In this connection, this very engineering solution is to be comprehensively studied.

A supercritical airfoil model was equipped with a multi-spark plasma system (Fig. 4) and tested in a wind tunnel for sets of basic flow and control parameters. Figs. 5-8 show results measured for chord-based $Re=3 \cdot 10^5$ and $7 \cdot 10^5$ and varying control parameters. In all figures, curves marked 'Ref.' show a reference case without flow control; designations of "0.2/200" type show pulse duration in milliseconds (first number) and pulse repetition rate in Hz (second number).

$$Re_c = 3.0 \times 10^5 \text{ case}$$

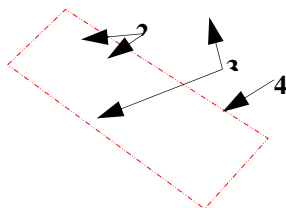


Fig. 5 shows lift and drag coefficient variations at high angles of attack.

Typically, plasma discharges result in growing maximal lift coefficients CL_{max} and stall angles that can be accompanied with drag coefficients reduction. Lift coefficient in the controlled case starts growing from $\alpha = 10^\circ$. Depending on plasma pulse duration/repetition rate combination, different increments of lift coefficient and stall angle were found. In the pre-stall region, all lift curves are very close to each other and diverge after a reference stall angle is reached. Within $\alpha = 14.5 \div 16^\circ$, an optimal τ/F combination can be found which produces maximal lift coefficient and stall angle increments. For $Re_C = 3.0 \times 10^5$, it is $\tau = 0.3$ ms, $F = 150$ Hz that results in $\Delta\alpha_{stall} = 1.5^\circ$ and $\Delta CL_{max} = CL_{max, Ctrl.} - CL_{max, Ref.} = 0.085$ (about 7%). Maximal CL increment under controlled conditions at the stall angle of $\alpha = 16.0^\circ$ compared to the post-stall value at the same angle of attack in a reference case is $\Delta CL_{\alpha=16.0^\circ} = CL_{\alpha=16.0^\circ, Ctrl.} - CL_{\alpha=16.0^\circ, Ref.} = 0.22$. Behavior of lift coefficients in the post-stall region in the controlled case is much smoother compared to an abrupt lift drop in the reference case.

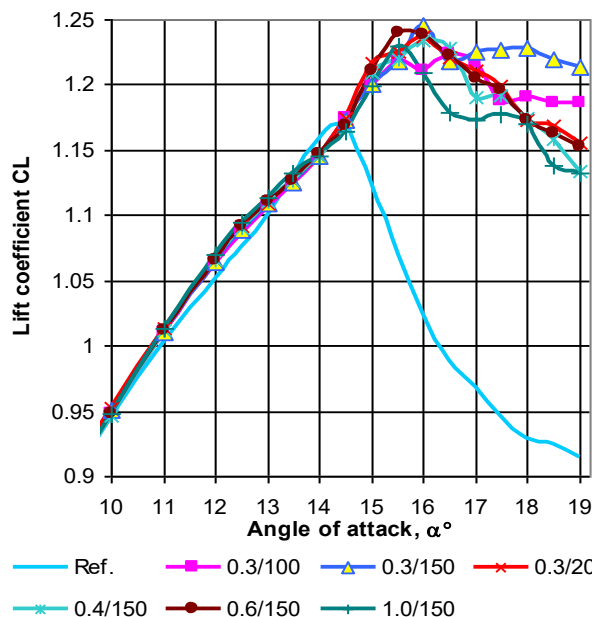


Fig. 5. Lift coefficient vs. angle of attack; $Re_C = 3.0 \times 10^5$

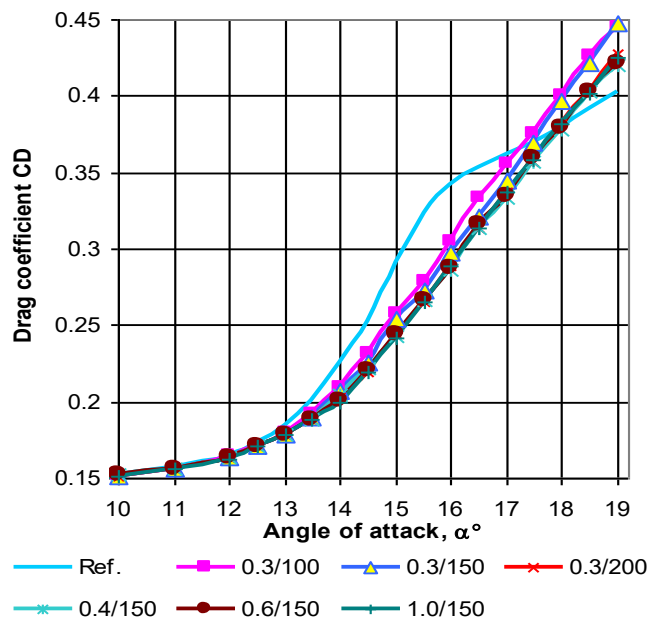


Fig. 6. Drag coefficient vs. angle of attack; $Re_C = 3.0 \times 10^5$

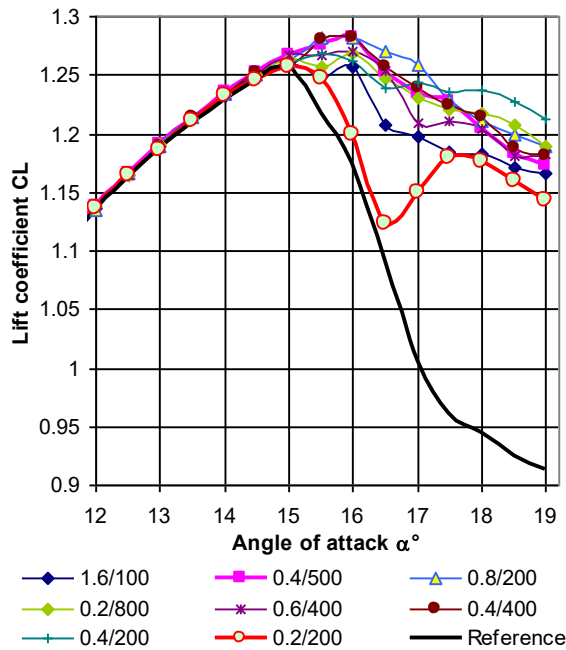


Fig. 7. Lift coefficient vs. angle of attack;
 $Re_C = 7.0 \times 10^5$

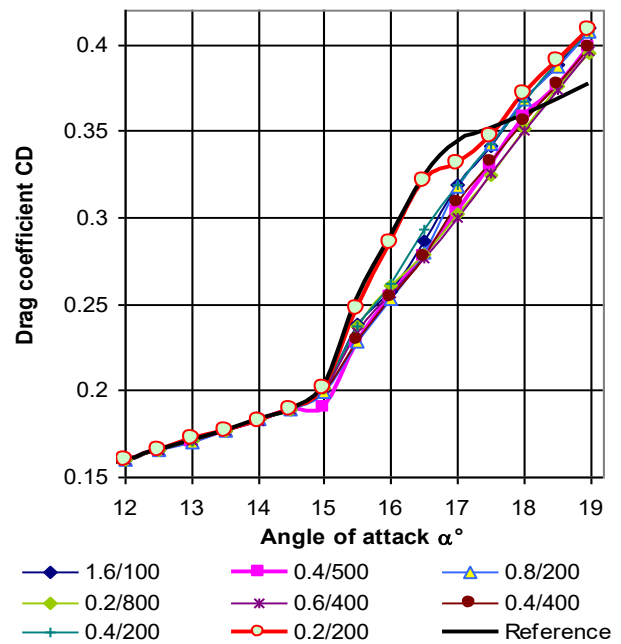


Fig. 8. Drag coefficient vs. angle of attack;
 $Re_C = 7.0 \times 10^5$

Drag reduction in the controlled case is found for $\alpha = 12.0 \div 17.0^\circ$. It looks like there is a threshold value of parameters above which all curves are very close to each other. At a stall angle in the controlled case, drag coefficient increment is $\Delta CD_{\alpha=16.0^\circ} \approx -0.056$ for $\tau/F = 0.4/150$.

Figs. 7 and 8 show that at higher Reynolds numbers, discharges also result in growing maximal lift and a stall angle accompanied with drag reduction. Lift coefficients in the controlled case grow from $\alpha = 14^\circ$ but their increment is smaller than at lower Reynolds numbers. Depending on a pulse duration/ repetition rate combination, different increments of lift coefficient and stall angle are found. In the pre-stall region, all lift curves are more close to each other and diverge after the stall angle of a reference case is reached. In a range of $\alpha = 15.0 \div 16^\circ$, an optimal τ/F combination is determined, which provides maximal lift and stall angle increments. At $Re_C = 7.0 \times 10^5$, these values are as follows, $\tau = 0.8$ ms, $F = 200$ Hz providing $\Delta\alpha_{stall} = 1.0^\circ$ and $\Delta CL_{max} = 0.025$. Maximal increment of lift coefficient obtained in the controlled case at $\alpha = 16.0^\circ$ stall angle compared to the CL at the same α which is in a post-stall area of a reference case is $\Delta CL_{\alpha=16.0^\circ} = 0.11$. And again, variation of $CL(\alpha)$ in post-stall region is smoother in the controlled case.

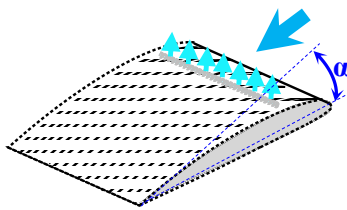
Drag reduction in the controlled case is found for $\alpha = 15.0 \div 17.5^\circ$. Here a threshold situation related to control parameters is not as evident as for the case of $Re_C = 3.0 \times 10^5$. At a stall angle in the controlled case, $\Delta CD_{\alpha=16.0^\circ} \approx -0.036$ for $\tau/F = 0.8/200$.

Supposedly, an optimal combination of τ/F for $Re_C = 7.0 \times 10^5$ was not found because of limited power of a high-voltage generator. The duty cycle of currently used generator is limited by the value of 20% ($\tau/T = 0.4 \times 10^{-3} \times 500 = 0.2$) which corresponds to the combination of $\tau/F = 0.4/500$; $\tau/F = 0.6/400$ exceeds this value and leads to the generator overloading. At the same time, the stall angle increment is 1.5° for lower Re_C and only 1.0° for $Re_C = 7.0 \times 10^5$. In addition, optimal power for CD control is greater at lower Reynolds numbers as shown in Table 2.2. That is why it was supposed that the energy released in the flow was insufficient at high Reynolds number. To verify this supposition, measurements at $Re_C = (8.5 \div 9.0) \times 10^5$ should be carried out with a more powerful generator.

Table 2.2. Optimal parameters for pulsating multi-spark flow control

Free-stream velocity U_{ts} , m/s	$Re_C \times 10^{-5}$	Stall angle $\alpha_{stall, C_{trl}}$	Pulse duration, ms	Pulse repetition rate, Hz	Optimal for:	Full power for the array, P_d , W	Aerodynamic power, P_{AD} , W	Relative AD power
22.4	3.0	16	0.3	150	CL	28	81	0.35
22.4	3.0	16	0.4	150	CD	31	81	0.38
38.0	5.0	16.5	0.4	200	CL	42	380	0.11
37.9	5.0	16.5	0.2	800	CD	67	349	0.19
55.1	7.0	16	0.8	200	CL, CD	83	1023	0.08

3. CONCLUSIONS



1. **SAP (Streamlined Aerodynamic Profile)** is an airfoil model with 12.5% relative thickness, similar to NASA TP-3579. **SAP2** is the model with an embedded linear array of pulsating multi-spark plasma discharges on its upper surface.
2. Measurements of aerodynamic characteristics of the SAP2 model controlled with a linear array of pulsating spark discharges showed growth of maximal values of lift coefficient by 8% and stall angle by 2.0° at different Reynolds numbers. At pre- and post-stall angles of attack the basic parameter affecting the lift is pulse repetition rate rather than total power consumed for plasma generation. Optimal combinations of pulse duration and pulse repetition rate differ for different Reynolds numbers. Higher Reynolds numbers need higher optimal pulse durations and higher pulse repetition rates.

3. To improve lift or drag, an optimal combination of τ & F is found to be different; it is the same only for the case of $Re_C = 7.0 \times 10^5$.

4. A kind of saturation is observed for drag coefficient increments, when after a certain energy is reached, its further growth does not reduce drag significantly and all the curves form a very dense bundle.

5. An impact of the pulsating multi-spark array on the post-stall region consists in a much slower or smoother lift falling with a growing angle of attack than in a reference case with an abrupt lift drop typical for supercritical airfoils.

6. A more powerful high-voltage generator with a wider range of pulsations parameters F and τ should be used for investigations at higher Reynolds numbers.

4. REFERENCES

- Yurchenko, N., Delfs, J. (1999), "Boundary layer control over an active ribletted surface" *In: Fluid Mechanics and its Applications*, eds. G. E. A. Meier and P. R. Viswanath, 53, Kluwer Academic Publishers, pp. 217-222.
- Rivir, R. B., Sondergaard, R., Bons, J. P., Yurchenko, N. (2004), "Control of Separation in Turbine Boundary Layers", *AIAA Paper-2004-2201*.
- Rozumnyuk, N., Zagumennyi, Ya. (2008), "Numerical Simulation of Near-Wall Turbulence Structure Affected by MW-Generated Point Plasma Discharges", *AIAA Paper-2008-1440*
- Yurchenko, N. F. (2008), "Speculation about near-wall turbulence scales", *Physica Scripta T132 014011*, 6 pp.
- Yurchenko, N., Esakov, I. (2011), "Interdisciplinary studies of flow control based on localized plasma discharges", *International J. of Fluid Mechanics Research*, v.38, pp. 272-289.
- Yurchenko, N. (2010), "Research strategy for active flow control based on distributed thermal fields", *International J. of Fluid Mechanics Research*, v. 57, No. 5, pp. 470-489.
- Concept of Fluid Motion Scale Control and Its Realization", *AIAA Paper 2015-1060*, 8 pp.
- Yurchenko, N. (2015), "Thermal riblets: conceptual approach to flow control", *Proc. European Drag Reduction and Flow Control Meeting – EDRFCM 2015, Cambridge, UK*, pp. 35-37.
- Yurchenko, N., Vynogradskyy, P., Kuzmenko, K. (2016) "Flow response to multi-spark and multi-jet flow actuation", *AIAA Paper AIAA 2016-1819*, 8 pp.

5. ACKNOWLEDGMENTS

This material is based upon work supported by the European Office of Aerospace Research and Development, AFOSR, AFRL under the Partner Project P-053 of STCU (Science and Technology Center in Ukraine) and CRDF GAP grants # UKE2-1508-KV-05, # UKE2-1518-KV-07, and #UKE2-31103-KV-12.